

Antinucleation Effect of the Polyethylene Block on the Polycaprolactone Block in ABC Triblock Copolymers

V. Balsamo* and A. J. Müller

Grupo de Polimeros USB, Departamento de Ciencia de los Materiales, Universidad Simón Bolívar, Aptdo. 89000, Caracas 1080-A, Venezuela

R. Stadler

Makromolekulare Chemie II, Universität Bayreuth, 95440 Bayreuth, Germany

Received February 26, 1998; Revised Manuscript Received June 15, 1998

ABSTRACT: Polystyrene-*block*-poly(ethylene-*co*-butylene)-*block*-poly(ϵ -caprolactone) triblock copolymers (SEC) were prepared by hydrogenating polystyrene-*block*-polybutadiene-*block*-poly(ϵ -caprolactone) triblock copolymers (SBC) previously prepared by sequential anionic polymerization. The effect of the crystallization of the polyethylene block (PE) upon cooling from a phase-segregated melt on the crystallization process of the adjacent polycaprolactone block (PCL) was investigated by means of differential scanning calorimetry and polarized optical microscopy. It was found that there was no nucleation effect of the PE block on the PCL block under controlled cooling conditions in the DSC. On the contrary, an antinucleation effect was detected when nucleation of the PCL block crystals within the SEC triblock copolymers was attempted. It was demonstrated that such an antinucleation effect was induced by the annealing of the polyethylene block crystals of the SEC copolymers. By the application of the successive self-nucleation and annealing technique (SSA) the possibility of producing a distribution of lamellar thickness within the PCL and the PE blocks of the SEC triblock copolymers was shown. These results, together with the spherulitic morphology displayed by the SEC copolymers with more than 50 wt.-% PCL, are consistent with previous morphological observations in SBC triblock copolymers. Those observations indicate that the chain stems within the lamellar crystals in the PCL blocks could be perpendicular to the interphase of the block copolymer domains, even though the crystallization occurred from a heterogeneous melt.

Introduction

The morphology and crystallization of AB diblock copolymers have been the subject of many recent investigations.^{1–11} However, there are only a few studies on ABC triblock copolymers with crystallizable blocks. In a previous work, Balsamo et al.¹² studied the thermal behavior of polystyrene-*block*-polybutadiene-*block*-poly(ϵ -caprolactone) SBC triblock copolymers. These copolymers exhibit microphase separation in the melt and crystallization of the polycaprolactone (PCL) block upon subsequent cooling if the molecular weight is high enough. The crystallization process of the PCL block is affected by the presence of the amorphous blocks. A general decrease of the crystallinity and a reduction of the equilibrium melting point (T_m°) with an increase of the $w_{PB}:w_{PCL}$ weight ratio were observed, indicating a thinning of the crystalline lamellae as a consequence of the chemical connection between the components. Similarly, an influence of the crystallization process on the microphase morphology was observed.¹³ The formation of undulate PCL lamellae with ellipsoidal core shell cylindrical microphases,¹³ when the PCL was the major component, and the building of polygonal core shell structures in a PS matrix are some of the examples of the peculiar morphologies obtained.

More recently we reported the hydrogenation of SBC triblock copolymers to obtain polystyrene-*block*-poly(ethylene-*co*-butylene)-*block*-poly(ϵ -caprolactone): i.e., SEC triblock copolymers with two crystallizable blocks, polyethylene (PE) and polycaprolactone (PCL).¹⁴ This was carried out in order to study the effect of the chain constraints on the crystallization process of the blocks as has been studied by Richardson et al.¹⁵ with a poly-

(ethylene oxide-*block*-methyl methacrylate) diblock copolymer. One of our objectives was to investigate the effect of the number of free ends on the crystallization of the components. As expected a marked depression of the PE block melting point and degree of crystallinity were observed compared to pure hydrogenated polybutadiene (HPB). This effect was less marked in the PCL block, which had at least one free end.

Previous works on semicrystalline block copolymers have concentrated on the study of the orientation of the crystallized polymer chains in diblock copolymers. It has been demonstrated that the final morphology depends on whether the crystallization takes place from a homogeneous or heterogeneous melt.^{4,5,8,16} There seems to be a consensus indicating that when crystallization proceeds from a homogeneous melt, the crystallization process determines the final morphology. In this case, the polymer chains possess a conventional perpendicular orientation of the chain stems with respect to the microdomain interface.^{9,16} On the other hand, other authors have deduced, from WAXS and SAXS data for oriented samples, that when crystallization takes place from a microphase-separated melt, chain stems are oriented parallel to the interphase.^{4,5,7} Additionally, the segregation level between the components and the glass transition of the amorphous block connected to the crystallizable block can influence the way in which the crystallized chain is oriented with respect to the microdomain interface.^{9,7,17} Rangarajan et al.⁹ showed that a weakly segregated poly(ethylene-*block*-head-to-head-propylene) forms spherulites although microphase separation precedes crystallization. The formation of spherulites indicated that the chains

are oriented perpendicular to the lamellar interface. With respect to the more complex ABC triblock copolymers, Balsamo et al.¹² showed that SBC triblock copolymers with a majority of the crystallizable component exhibit well-defined spherulites. Furthermore, these materials had a dependence of the equilibrium melting point on the composition. These facts suggested a perpendicular array of the crystallized chain stems with respect to the microdomain interface.

When a system is composed of two or more crystallizable components, it is interesting to investigate the effect of the crystallization of each block on the other: for example, whether there will be nucleation of the second component by the first, as has been observed in some polymer blends,^{18,19} or whether the first component, on the contrary, disturbs the crystallization of the other component, as has been reported in some cases when there are specific interactions between the components.^{20,21} SEC triblock copolymers with a minor PCL fraction showed fractionated crystallization even though the PE block had already crystallized.¹⁴ This result and the general decrease of the PCL crystallization temperature in SEC compared with SBC triblock copolymers were the first evidences to suggest that there is no nucleation effect of the PE block on the crystallization of the PCL block.¹⁴ Such lack of nucleation effect of the PE block on the PCL block is surprising since it has been reported by Kalfoglou²² that the PCL crystallizes to a larger extent in the presence of small LDPE crystals probably due to an epitaxial crystallization of PCL on LDPE. It was therefore aim of this work to study the effect of the crystallization of the PE block on the crystallization process of the PCL block.

We also studied in this paper the changes in the thickness distribution of the crystallites for the different triblock copolymers prepared. Here we use the successive self-nucleation and annealing (SSA) technique. This technique was recently developed by Müller et al.²³ to study molecular segregation during crystallization by DSC. The technique consists of a series of successive self-nucleation and annealing steps that are designed to enhance potential molecular fractionation during crystallization. Such fractionation can commonly occur in polymers that contain a small percent of chain branches or in linear polymers whose crystallization is sensitive to differences in molecular lengths (i.e., polydispersity) as the temperature is varied.

Experimental Section

Materials. The polystyrene-*block*-poly(ethylene-*co*-butylene)-*block*-poly(ϵ -caprolactone) (SEC) triblock copolymers used in the present study were obtained through hydrogenation of polystyrene-*block*-polybutadiene-*block*-poly(ϵ -caprolactone) (SBC) triblock copolymers with high 1,4-PB units using the Wilkinson catalyst. The details are described elsewhere.¹⁴ The molecular characteristics of the samples are presented in Table 1. A poly(ethylene-*co*-butylene)-*block*-poly(ϵ -caprolactone) (EC) diblock copolymer and a poly(ϵ -caprolactone) homopolymer (PCL) were used as reference materials.

Differential Scanning Calorimetry (DSC). The samples were encapsulated in aluminum pans and high purity dry nitrogen was used as an inert atmosphere in a Perkin-Elmer DSC7. The instrument was calibrated with chloroform and naphthalene. A preliminary thermal characterization was performed by heating and cooling the materials at 20 °C/min after the samples were held in the melt at 140 °C for three minutes, to erase all previous thermal history.

Self-Nucleation Experiments. To analyze the crystallization behavior of the materials under study we performed self-

Table 1. Molecular Characteristics of the SEC Triblock Copolymers

polymer ^a	$M_n \times 10^{-3}/$ $\text{g} \cdot \text{mol}^{-1}$ ^b	M_w/M_n	ethyl branches/mol %
PCL	83	1,50	
S ₅₇ E ₂₇ C ₁₆	137	1,12	3,2
S ₂₇ E ₃₇ C ₃₆	132	1,20	2,3
S ₃₅ E ₁₅ C ₅₀	150	1,22	2,9
S ₂₇ E ₁₅ C ₅₈	219	1,30	2,6
E ₂₀ C ₈₀	68	1,25	3,5

^a The subindices represent the weight percent of each component. ^b Determined from ¹H NMR and GPC calibrated with PS standards.

nucleation (SN) experiments.²⁴ These experiments involved the partial melting of a crystalline "standard" state followed by recrystallization using as nuclei the crystal fragments produced in the partial melting stage. The detailed procedure is described as follows:

(a) Erasure of Previous Thermal History. The sample was kept at 140 °C for 3 min. This initial melting leaves only temperature-resistant heterogeneous nuclei of unknown nature.

(b) Creation of the Initial "Standard" State. The sample was cooled at a rate of 20 °C/min down to -110 °C and held for 10 min at that temperature.

(c) Self-Nucleation. The sample was heated at 20 °C/min up to a selected self-seeding temperature (T_s) and it was held at that temperature for 6 min. This results in partial melting and, depending on T_s , in the annealing of unmelted crystals.

(d) Final Crystallization. Subsequent cooling at 20 °C/min from T_s down to -110 °C is allowed.

(e) Final Melting. Subsequent heating is done at 20 °C/min from -110 up to +140 °C. Depending on the T_s , self-nucleation and/or annealing of the remaining crystals can occur.²⁴

Successive Self-Nucleation and Annealing (SSA) Technique.²³ A more detailed study of the effect of the PE crystals on the PCL crystallization was attempted using this method. As mentioned before, this technique enhances the potential molecular fractionation that can occur during crystallization, while encouraging annealing of the unmelted crystals at each stage of the process, so that small effects can be magnified.

Steps a–c of the SN method were repeated as the first part of this experiment, and then the following steps were performed.

(d) Cooling from T_s . The sample was cooled from T_s down to -110 °C at 20 °C/min and held at that temperature for 10 min.

(e) Heating to a New T_s . The sample was heated once again at 20 °C/min, but this time up to a T_s which was 5 °C lower than the previous T_s and held at that temperature for 6 min. This means that the unmelted crystals at T_s will anneal and some of the melted species will isothermally crystallize (after being self-nucleated by the unmelted crystals) while the rest of the molten crystallizable chain segments will only crystallize during the subsequent cooling from T_s .

(f) Steps d and e Repeated at Increasingly Lower T_s . The differences in T_s were always kept constant at 5 °C.

(g) Final Melting. The sample was heated from -110 up to +140 °C at 20 °C/min.

The SSA experiment is illustrated in Figure 1, with T_s being lowered at 5 °C intervals with respect to the previous step. The chosen T_s range was 90–40 °C.

Results and Discussion

Before any thermal analysis was performed in the triblock copolymers, SN tests were carried out in the PCL homopolymer in order to determine the corresponding self-nucleation domains. According to the location of T_s in the melting endotherm, Fillon et al.²⁴ defined the following domains.

Domain I: In this temperature range, the remaining nuclei corresponds to heterogeneous nuclei i.e., ther-

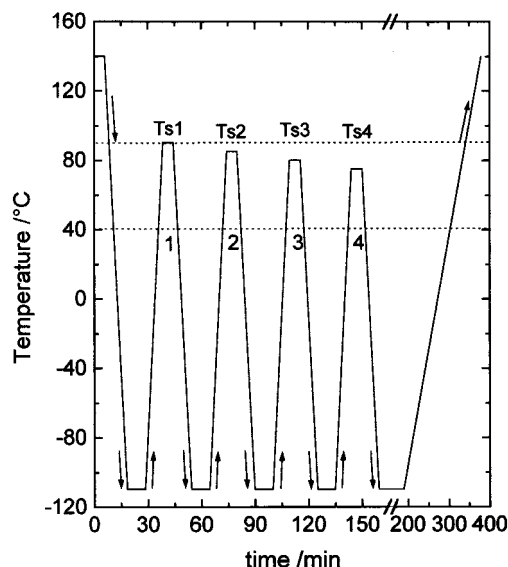


Figure 1. Schematic representation of successive self-nucleation and annealing (SSA) thermal treatments. The dotted lines define the melt range within the T_s temperatures were varied.

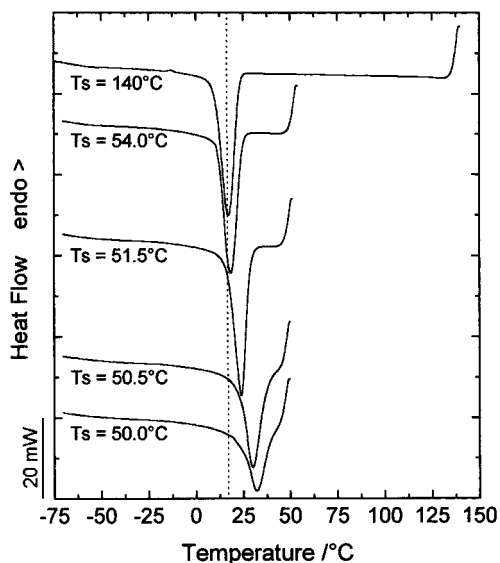


Figure 2. Cooling DSC scans of PCL at 20 °C/min after self-nucleation (SN) at T_s .

mally stable nuclei present in the melt. Upon cooling, recrystallization takes place always at the same temperature.

Domain II: In this T_s range, the concentration of remaining crystals fragments varies dramatically. Small variations of T_s result on subsequent cooling in significant shifts of the crystallization peak to higher temperatures.

Domain III: In this range, incomplete melting takes place. Considerable annealing of the unmelted material occurs.

Figure 2 shows representative crystallization exotherms of PCL after the partial or total melting at various self-seeding temperatures (T_s), and Figure 3 presents the variation of the peak crystallization temperature (T_c) with T_s . A reduction of T_s produces a shift of the crystallization temperature to higher temperatures. This change, clearly seen in Figure 3 at temperatures lower than 60 °C, is attributed to a self-nucleation process promoted by the remaining stabilized

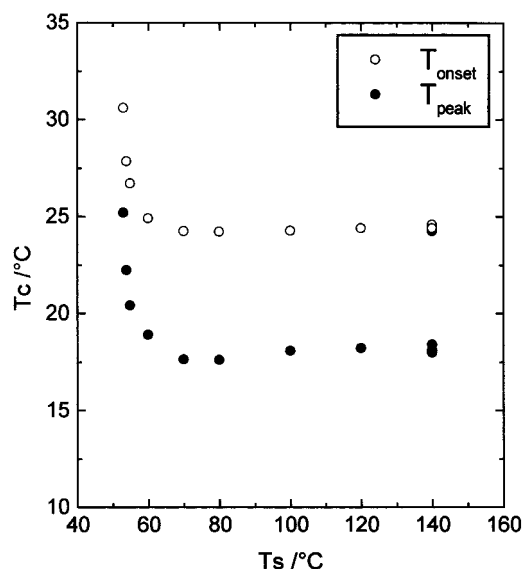


Figure 3. Change of T_c with T_s for the PCL homopolymer during the self-nucleation (SN) treatments.

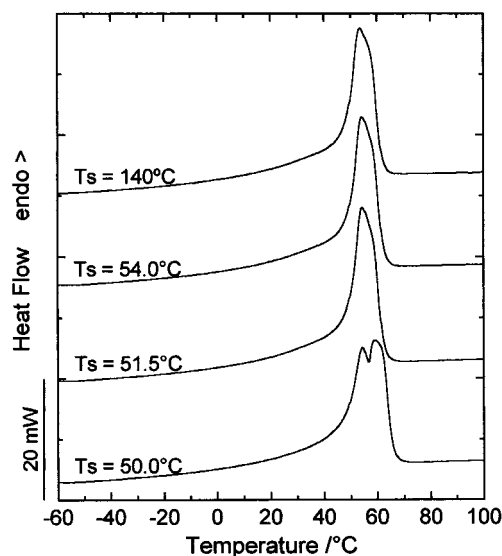


Figure 4. Heating DSC scans of PCL at 20 °C/min after Self-Nucleation at T_s and recrystallization.

crystal fragments at T_s . This behavior is typical of domain II, in which small variations of T_s changes dramatically the concentration of remaining crystals fragments. At temperatures lower than 50.5 °C recrystallization takes place almost immediately upon cooling.

To establish the limit between domains II and III, the subsequent melting behavior was analyzed (see Figure 4). On remelting, after crystallization from a specific self-seeding temperature, an additional high-temperature endotherm becomes apparent if T_s is lower than 50.5 °C. The appearance of a higher melting temperature peak indicates that at that T_s , annealing of the unmelted crystals has taken place; i.e., domain III has been reached, and this peak becomes more important as T_s decreases.²⁴

On the basis of results presented above we can define the self-nucleation domains for the PCL homopolymer as depicted in Figure 5. The transition between the domains is occurring at somewhat lower temperatures with respect to the relative positions of the melting peak and its high-temperature tail when compared to the analogous results obtained by Fillon et al.²⁴ in isotactic

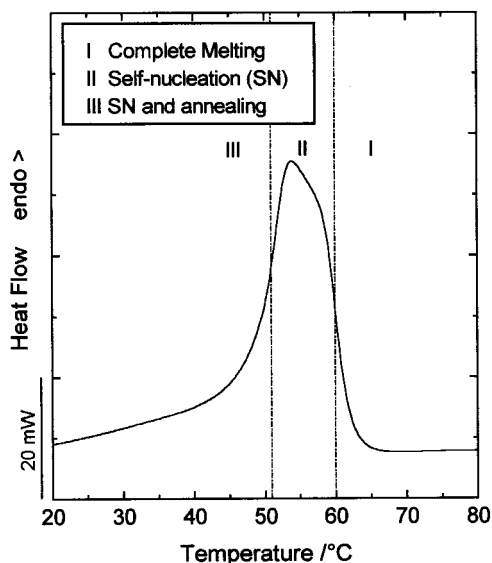


Figure 5. Definition of the self-nucleation regimes for the PCL homopolymer under study.

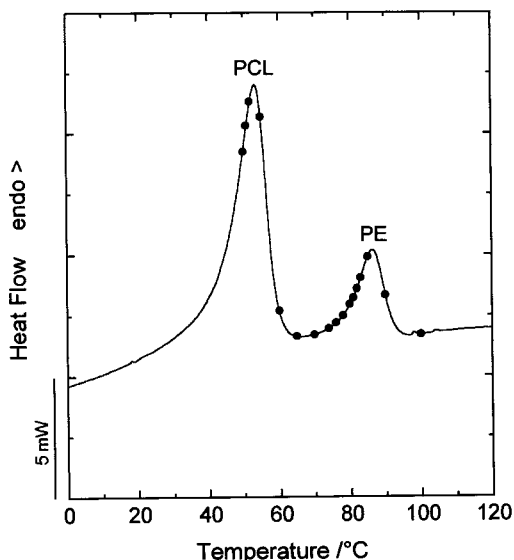


Figure 6. Heating DSC scans of $S_{35}E_{15}C_{50}$ at 20 °C/min. The solid circles indicate the different self-seeding temperatures T_s at which SN tests were performed.

polypropylene. The PCL crystals have a pronounced tendency to melt since in order to produce annealed crystals, the T_s temperature has to be lower than 50.5 °C. This effect is currently under investigation in our laboratory, and it may be linked to the narrow molecular weight distribution of the PCL as opposed to the wide polydispersity of the iPP samples of Fillon et al.²⁴

On the basis of the self-nucleation domains found for the PCL homopolymer, SN tests were carried out in the hydrogenated triblock copolymers. The self-seeding temperature was varied from 140 down to 50 °C. It should be noted that at T_s temperatures higher than 60 °C the PCL is in domain I, i.e., the crystals are completely melted. For the hydrogenated triblock copolymers, depending on the magnitude of T_s , partial melting and/or annealing of PE crystals occurs. Figure 6 shows the self-seeding temperatures at which SN tests were performed for $S_{35}E_{15}C_{50}$. In Figure 7 the DSC cooling scans for $S_{35}E_{15}C_{50}$ are shown, after the samples were held at different T_s for 6 min.

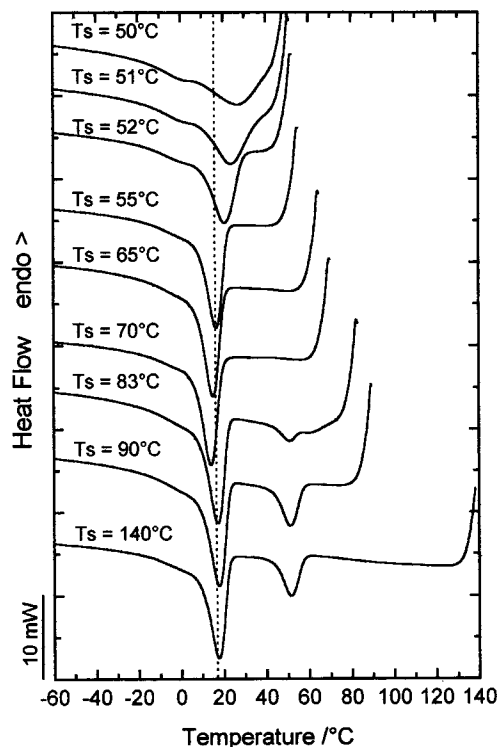


Figure 7. Cooling DSC scans of $S_{35}E_{15}C_{50}$ at 20 °C/min after self-nucleation at T_s .

When the $S_{35}E_{15}C_{50}$ is cooled from 140 °C (where the sample is completely molten in domain I), two crystallization exotherms can be clearly observed. The first one at higher temperatures (between approximately 60 and 40 °C) corresponds to the crystallization of the PE block within the copolymer. Following the cooling scan to lower temperatures, the PCL block crystallizes in the second exotherm with a peak crystallization temperature of 17.5 °C, at temperatures well below the crystallization temperatures of the PE block. The crystallization of neat PCL at the same cooling conditions was observed around 18 °C according to Figures 2 and 3. Therefore, the PE block that has crystallized before during the scan (at higher temperatures) does not nucleate the PCL block.

As the T_s temperature is lowered in Figure 7, the PE block will be partially molten and only part of it will crystallize upon cooling (e.g. $T_s = 83$ °C curve in Figure 7). Below a T_s of 70 °C the crystallization exotherm of the PE block completely disappears, since it has already finished its crystallization, and a peculiar effect on the crystallization of the PCL block can be observed.

The influence of T_s on T_c for the PCL block after self-nucleation is shown in Figure 8a for $S_{35}E_{15}C_{50}$. This sample exhibits a remarkable behavior; it exhibits a temperature range (85–52 °C) where a reduction of the PCL block crystallization temperature is observed. Similar results were obtained with another triblock copolymer, the $S_{27}E_{15}C_{58}$, and they can be seen in Figure 8b.

To investigate the origin of the reduction of the PCL block crystallization temperature in the range showed, we performed the same experiment in the non-hydrogenated block copolymers, i.e., where the PCL block is connected to polybutadiene instead of polyethylene. Figure 9 presents a comparison of the results for $S_{27}B_{15}C_{58}$ and $S_{27}E_{15}C_{58}$. The non-hydrogenated sample shows no reduction of the crystallization temperature

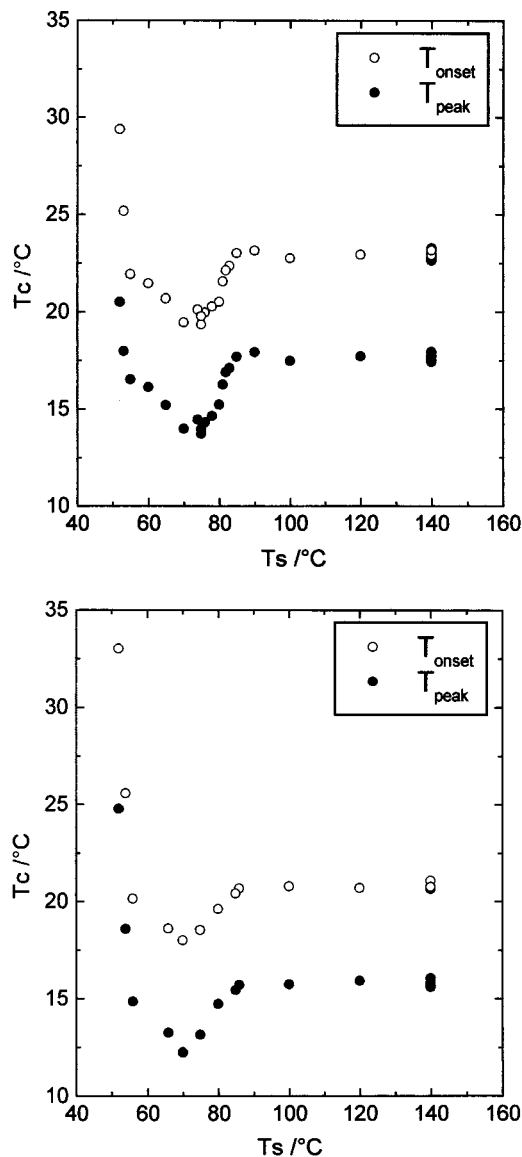


Figure 8. Change of T_c with T_s for (a) $S_{35}E_{15}C_{58}$ (above) and (b) $S_{27}E_{15}C_{58}$ (below) during SN treatments.

of the PCL block, and a normal self-nucleation behavior as in pure PCL (Figure 3) is observed. This leads to the conclusion that the observed depression of the crystallization temperature of the PCL block is an effect inherent to the SEC triblock copolymers. It must be stressed that in both kinds of triblock copolymers (SEC and SBC) the PCL block crystallizes in an already microphase-separated system with a PS block that is glassy at the temperature where PCL crystallization starts.^{12,14}

The PCL crystallization temperatures were depressed in the SEC copolymers as compared to the SBC copolymers in the subsequent cooling runs from T_s temperatures that correspond to the lowest melting temperature tail of the PE block (see Figure 6). At these T_s temperatures, annealing of the thinner or more defective PE crystals takes place. This fraction of thinner crystals is probably located near the interface with the polycaprolactone block. It is probable that the PCL chains directly attached to PE chains at the interface experience diffusion problems to reach active nuclei in view of topological constraints. The annealing of these thinner crystals must be responsible for the difficulties experienced by the PCL block during nucleation in the

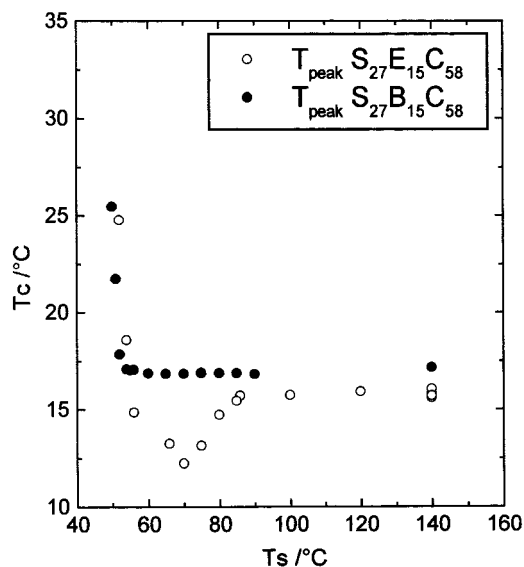


Figure 9. Comparison of the self-nucleation result for the hydrogenated and non-hydrogenated $S_{27}B_{15}C_{58}$ triblock copolymer.

subsequent cooling scan from T_s . Since this effect leads to a reduction of the $T_{c,PCL}$, we have termed this phenomenon the “**antinucleation effect**”. It is appropriate to point out that all polymers were purified in the same way. Therefore, the variation of T_c cannot be attributed to a change in the number of nuclei. As a matter of fact, both types of copolymers (SBC and SEC) formed well-developed spherulites (with approximately equal number per unit volume) upon cooling from T_s in the range defined as domain I in Figure 5. (see below). A change in growth geometry for the PCL block is therefore also ruled out.

The antinucleation effect found is opposite to what has been observed in PE/PCL blends by Kalfoglou.²² In the case of PE/PCL blends, there are no chemical bonds at the interface between the two components. It is therefore possible that epitaxial crystallization of the PCL occurs upon cooling on the surface of the PE crystals in the case of physical blends. In our case the reduction of the mobility of the PCL block is promoted by the chemical link between the components, and probably the thinnest PE block crystal fraction corresponds to the crystallization of the chain segments that are nearer to the interfacial chemical link. This antinucleation effect would be comparable to the inhibited nucleation showed by some filled polymers, caused by strong interactions between the polymer and the filler, which reduce the mobility of the polymer in the melt.^{25,26}

To study the antinucleation effect in more detail we performed successive self-nucleation and annealing (SSA) experiments.²³ While each point obtained from self-nucleation experiments (in Figures 8 and 9) is a single result after a standard cooling from T_s ; the SSA experiments have the advantage that the thermal history of the material in the previous T_s , after the self-nucleation, has been preserved. This means that in a SSA experiment the sample has a family of annealed crystals fractions, which are the product of a molecular fractionation. The result of this experiment, described in Figure 1, is shown in Figure 10 for $S_{27}E_{15}C_{58}$ compared with the SN experiment. In the case of SSA, the crystallization temperature plotted in Figure 10 is the crystallization upon cooling from T_s at each step of the successive procedure indicated in Figure 1 and

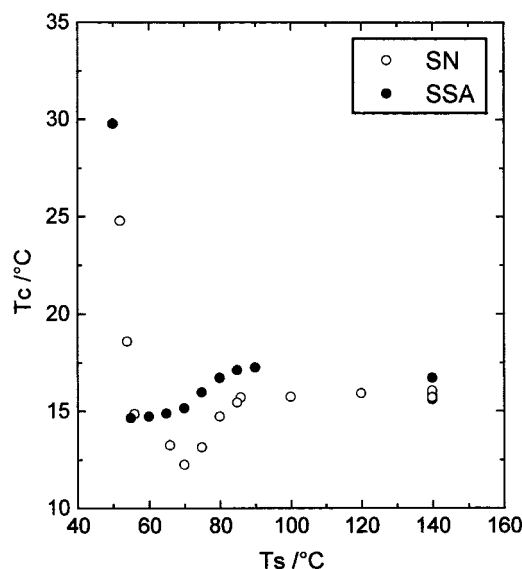


Figure 10. Comparison of the SN and SSA thermal treatments for $S_{27}E_{15}C_{58}$.

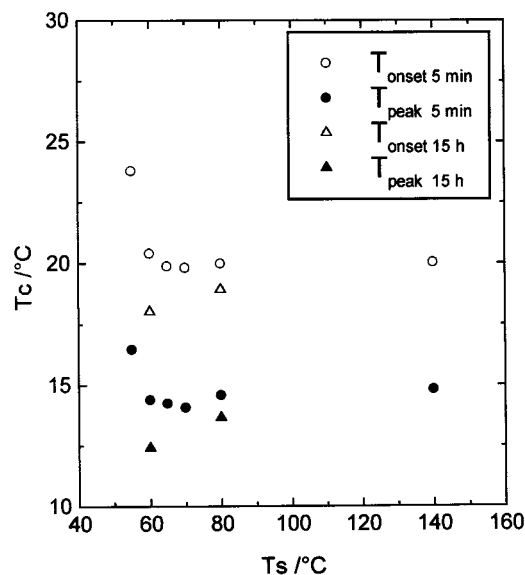


Figure 11. Change of T_c with T_s for $S_{27}E_{37}C_{36}$ after SN treatment.

corresponding to step d described in the Experimental Section. Again a reduction of the crystallization temperature is observed with a decrease of T_s , but no increase is observed until self-nucleation of the PCL occurs; i.e., a sharp and somewhat symmetrical minimum like that obtained after the SN experiments was not present in the SSA results. This is due to the fact that in the SSA experiments at the lowest T_s temperatures (before self-nucleation of the PCL, i.e., 60 °C), where almost no annealing of the PE occurs, the previously annealed PE crystals (at higher T_s in previous SSA steps) are still present, disturbing the PCL crystallization, i.e., “antinucleating” the PCL. On the other hand, in the SN experiments the thermal history of each step is erased, so that in the range 55–65 °C no significant annealing of PE crystals occurred. Similar results were obtained with $S_{35}E_{15}C_{50}$.

The antinucleation effect was, however, not present in the same time scale in all investigated triblock copolymers. Figure 11 shows that for $S_{27}E_{37}C_{36}$ only after 15 h at T_s the antinucleation effect was apparent

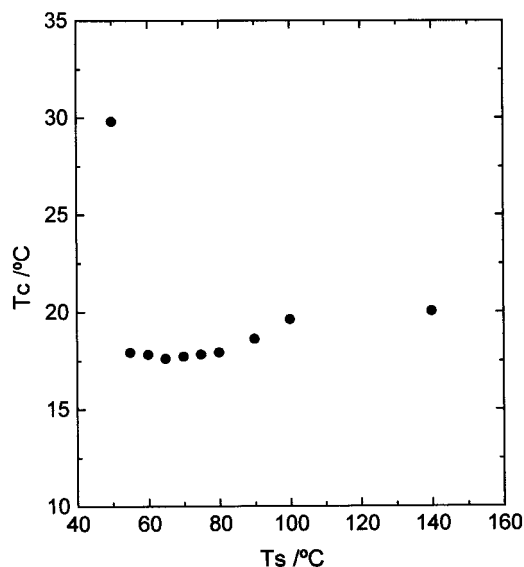


Figure 12. Change of T_c with T_s for $E_{20}C_{80}$ after SSA treatment.

on the subsequent cooling run. In a previous work, where this copolymer was analyzed, it was detected that the PCL block of $S_{27}E_{37}C_{36}$ exhibited a normal crystallization peak at 14 °C and a low temperature shoulder at around –3 °C.¹⁴ This low temperature shoulder was attributed to a fractionated crystallization process produced by the confinement of the PCL component in very small domains. The fraction of PCL that does not crystallize at high temperatures probably makes easier the crystallization of the rest of the PCL, despite the annealed PE crystals. For that reason, the effect on the crystallization temperature of PCL is observed only after a long annealing time of the PE crystals, i.e., when the PE lamellae are thicker. Another possible explanation could be a change of the micromorphology with the composition. It is possible that the particular domain array would make easier the formation of the PCL crystals. The morphology of the SEC triblock copolymers is still under investigation.

The only EC diblock copolymer used in this work also exhibits the antinucleation effect (see Figure 12) but to a minor extent. The absence of the glassy PS block at the crystallization temperatures of the PE block and the PCL block probably makes easier the annealing of the PE crystals than in $S_{27}E_{37}C_{36}$, but on the other hand it also makes easier the crystallization of the PCL block, since the PCL chains will have a free end during crystallization. Furthermore, the higher PCL content in the $E_{20}C_{80}$ diblock copolymer could also explain the observed behavior.

As a part of the SSA experiment, a final heating scan was registered, as described in the experimental part (step g). As mentioned before, the SSA technique allows melt/melt and melt/solid segregation to occur during thermal cycles that promote self-nucleation, crystallization, and annealing processes.²³ In this way, qualitative information about the distribution of lamellar thickness obtained after successive annealings, if molecular segregation occurs during crystallization, can be obtained. The results gathered by Müller et al.²³ in ethylene/ α -olefin copolymers confirm that the SSA technique provides better fractionation than other similar techniques based on step crystallization. Therefore, from the final heating scan of the SSA test an idea about the

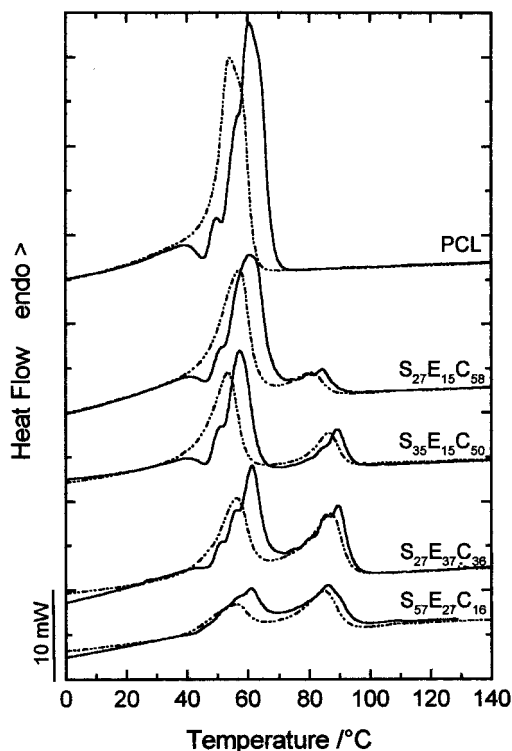


Figure 13. (—) Final heating DSC scans at 20 °C/min after the SSA treatment. (---) Standard heating after a dynamic crystallization at 20 °C/min.

distribution of lamellar thicknesses in the sample can be obtained.

Figure 13 shows the final heating scan after SSA for all investigated samples. After the SSA treatment, the neat PCL exhibits a complex fusion endotherm with at least four shoulders or peaks. Such multimodal melting can be attributed to the melting of four different mean lamellar thicknesses induced by the SSA treatment. The reason the PCL is capable of undergoing such molecular segregation during crystallization is probably connected to its residual polydispersity.

The effect of annealing is very clear when melting after SSA is compared to the melting after a simple controlled cooling at 20 °C/min (Figure 13). The peak melting point of the PCL increases by nearly 10 °C after the SSA treatment. The results of the SSA treatment in the SEC triblock copolymers are also presented in Figure 13. The appearance of multiple peaks corresponding to the melting of polyethylene and polycaprolactone blocks can be observed, indicating that the formation of lamellae of varied thickness within the confinement of the microdomains is also possible. This is a surprising result if one considers that some of the blocks must crystallize in extremely confined spaces within the microphase-separated domains of the block copolymers. Even in these conditions they are capable of undergoing molecular segregation during crystallization and annealing when the SSA treatment is applied. The location of the PE block next to the PS glassy block and the absence of free ends might explain the comparatively poor annealing of the PE blocks as compared to the PCL blocks, if the small increase in melting peak temperature after SSA of the PE blocks is considered.

The question of how the different crystallites can be arranged in the microdomains emerges. To clarify this point we followed the crystallization of the samples under the polarizing microscope. No discernible bire-

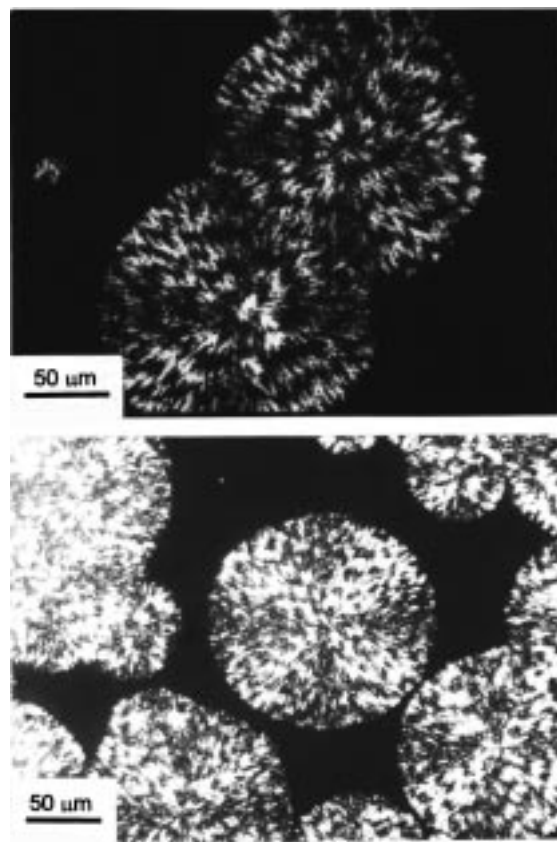


Figure 14. Spherulites formed after isothermal crystallization at 42 °C for (a) $S_{27}E_{15}C_{50}$ (above) and (b) $S_{27}E_{15}C_{58}$ (below).

fringe patterns were observed during cooling until the PCL block crystallizes, even though the PE block crystallized at higher temperatures during cooling than the PCL block. $S_{27}E_{15}C_{58}$ and $S_{35}E_{15}C_{50}$ are able to grow well-defined spherulites during isothermal crystallization (see Figure 14b), even though, at that crystallization temperature, the PS block had already vitrified and the PE block had already crystallized. The formation of such spherulites with the characteristic Maltese cross pattern confirms a radial growth of crystalline lamellae with a tangential array of the PCL chain segments. A banding phenomenon could be additionally observed similar to that presented by SBC triblock copolymers (Figure 14a).¹²

The question of how the multiple crystallites can be accommodated in the microdomains within the spherulite remains open, specially since spherulite formation for these triblock copolymers is driven by the PCL block crystallization even though the other two blocks have already vitrified (PS block) and crystallized (PE block). In the past few years, intensive investigations about the interplay between crystallization and microphase separation in semicrystalline diblock copolymers have been performed. It has been shown that the array of the crystallites within the microdomains depends strongly on whether the crystallization proceeds from a heterogeneous or a homogeneous melt. Several authors have shown in semicrystalline AB diblock copolymers with a lamellar micromorphology that, when crystallization proceeds from a heterogeneous melt, the chains fold with stems parallel to the microdomains interface.^{4,5,7} In contrast, when crystallization proceeds from a homogeneous melt, the chains fold with stems perpendicular to the microdomain interface.^{17,8}

In our samples, crystallization takes place from a heterogeneous melt, in which the polystyrene has vitrified;¹⁴ however, the observation of well-defined spherulites such as in SBC triblock copolymers and the change of the equilibrium melting point with composition, as well as the observed dependence of the microphase morphology with the crystallization temperature in SBC triblock copolymers,¹² leads one to think of a conventional array of chain folds with stems perpendicular to the microdomain interface. The SSA experiments additionally showed the possibility of the coexistence of multiple lamellar thicknesses (see Figure 13). How these multiple crystallites can be stacked in the semicrystalline domains is now the subject of our investigation. A possibility that cannot be discarded due to the lack of more experimental evidences is a fractionation of the crystallization in different microdomains of varied size due to molecular heterogeneity within the relatively narrow molecular weight distribution of these materials.

From Figure 13 other observations can be made. In $S_{27}E_{37}C_{36}$ there is a better definition of the melting peaks than in the other materials. This agrees with the results of self-nucleation experiments, which showed a less disturbed crystallization of the PCL block, i.e., a less marked antinucleation effect. This could be due, as mentioned before, to changes in the micromorphology. On the other hand, in $S_{57}E_{27}C_{16}$, which has a high polystyrene content, there is a lesser definition of the multiple melting peaks, indicating as expected a more restricted crystallization due to the confining of the PCL to small microdomains.

Conclusions

An antinucleation effect of the PCL block was detected by self-nucleation experiments of SEC triblock copolymers. By comparison with the absence of a similar effect in the parent non-hydrogenated versions of the same block copolymers, it was possible to ascertain that the antinucleation effect was caused by the annealing of the PE block crystals at a temperature T_s , before the crystallization of the PCL block at lower temperatures during subsequent cooling from T_s . In particular, the annealing of the lowest melting point crystals within the distribution present in the PE block was identified as the main cause of the effect. Such crystals may be the closer ones to the interface between the PCL and the PE where the covalent bonds linking both blocks are located.

The SSA technique revealed that, even within the confinement of the phase separated domains of the SEC triblock copolymers, molecular segregation and annealing can take place and a distribution of melting points can be generated. Such distribution can arise from a distribution of lamellar thicknesses formed during the SSA process within the copolymer microdomains.

The formation of spherulites displayed by the SEC copolymers with more than 50 wt % PCL, as well as

the SSA results, is consistent with previous morphological observations in SBC triblock copolymers that probably indicate that the chain stems within the lamellar crystals in the PCL blocks could be perpendicular to the interface of the block copolymer domains even though the crystallization occurred from a heterogeneous melt.

Acknowledgment. V.B. and A.J.M. acknowledge the support of CONICIT through grant S1-96001934 and of the "Decanato de Investigación y Desarrollo" of the USB through Grant GID-DID-G02. R.S. wishes to express thanks for the financial support of the joint project BSF/BMFT No. 3A312440993F and Stiftung Innovation Rheinland-Pfalz.

References and Notes

- (1) Heuschen, J.; Jérôme, R.; Teyssié P. *J. Polym. Sci., B: Polym. Phys.* **1989**, 27, 523.
- (2) Whitmore, M. D.; Noolandi, J. *Macromolecules* **1988**, 21, 1482.
- (3) DiMarzio, E. A.; Guttman, C. M.; Hoffman, J. D. *Macromolecules* **1980**, 13, 1194.
- (4) Cohen, R. E.; Bellare, L.; Drzewinski, M. A. *Macromolecules* **1994**, 27, 2321.
- (5) Douzinas, K. C.; Cohen, R. E. *Macromolecules* **1992**, 25, 5030.
- (6) Nojima, S.; Kato, K.; Yamamoto, S.; Ashida, T. *Macromolecules* **1992**, 25, 2237.
- (7) Hamley, I. W.; Fairclough, J. P. A.; Terrill, N. J.; Ryan, A. J.; Lipic, P. M.; Bates, F. S.; Towns-Andrews, E. *Macromolecules* **1996**, 29, 8835.
- (8) Rangarajan, P.; Register, R. A.; Adamson, D. H.; Fetters, L. J.; Bras, W.; Naylor, S.; Ryan, A. J. *Macromolecules* **1995**, 28, 1422.
- (9) Rangarajan, P.; Register, R. A.; Fetters, L. J.; Bras, W.; Naylor, S.; Ryan, A. J. *Macromolecules* **1995**, 28, 4932.
- (10) Drzewinski, M. A. *Macromol. Symp.* **1995**, 91, 107.
- (11) Gan, Z.; Zhang, J.; Jiang, B. *J. Appl. Polym. Sci.* **1997**, 60, 1793.
- (12) Balsamo, V.; von Gyldenfeldt, F.; Stadler, R. *Macromol. Chem. Phys.* **1996**, 197, 3317.
- (13) Balsamo, V.; Stadler, R. *Macromol. Symp.* **1997**, 117, 153.
- (14) Balsamo, V.; Müller, A. J.; von Gyldenfeldt, F.; Stadler, R. *Macromol. Chem. Phys.* **1998**, 199, 1063.
- (15) Richardson, P. H.; Richards, R. W.; Blundell, D. J.; MacDonald, W. A.; Mills, P. *Polymer* **1995**, 36, 3059.
- (16) Rangarajan, P.; Register, R. A.; Fetters, L. J. *Macromolecules* **1993**, 26, 4640.
- (17) Hamley, I.; Fairclough, J. P. A.; Ryan, A. J.; Bates, F. S.; Towns-Andrews, E. *Polymer* **1996**, 37, 4425.
- (18) Galeski, A.; Bartczak, Z.; Pracella, M. *Polymer* **1984**, 25, 1323.
- (19) Bartczak, Z.; Galeski, A.; Krasnikova, N. P. *Polymer* **1987**, 28, 1627.
- (20) Bartczak, Z.; Galeski, A.; Martuscelli, E.; Janik, H. *Polymer* **1985**, 26, 1843.
- (21) Bartczak, Z.; Galeski, A.; Pracella, M. *J. Appl. Polym. Sci.* **1994**, 54, 1513.
- (22) Kalfoglou, N. K. *J. Appl. Polym. Sci.* **1983**, 28, 2541.
- (23) Müller, A. J.; Hernández, Z. H.; Arnal, M. L.; Sánchez, J. J. *Polym. Bull.* **1997**, 39, 465.
- (24) Fillon, B.; Wittmann, J. C.; Lotz, B.; Thierry, A. *J. Polym. Sci., B: Polym. Phys.* **1993**, 31, 1383.
- (25) Cheng, S.; Shanks, R. A. *J. Appl. Polym. Sci.* **1993**, 47, 2149.
- (26) Turturro, G.; Brown, G. R.; St-Pierre, L. E. *Polymer* **1984**, 25, 659.

MA980305M